JCTC Journal of Chemical Theory and Computation

Article

pubs.acs.org/JCTC

Advances in Charge Displacement Analysis

Giovanni Bistoni,*[,†,‡] Leonardo Belpassi,[‡] and Francesco Tarantelli[†,‡]

[†]Dipartimento di Chimica, Biologia e Biotecnologie, Università di Perugia, Via Elce di Sotto 8, 06123 Perugia, Italy

[‡]Istituto di Scienze e Tecnologie Molecolari del CNR, Via Elce di Sotto 8, 06123 Perugia, Italy

Supporting Information

ABSTRACT: We define new general density-based descriptors for the quantification of charge transfer and polarization effects associated with the interaction between two fragments and the formation of a chemical bond. Our aim is to provide a simple yet accurate picture of a chemical interaction by condensing the information on the charge rearrangement accompanying it into a few chemically meaningful parameters. These charge displacement (CD) parameters quantify the total charge displaced upon bond formation and decompose it into a charge transfer component between the fragments and charge rearrangements taking place within the fragments. We then show how the new parameters can be easily calculated using the well-known CD function, which describes the charge flow along a chosen axis accompanying the formation of a bond. The approach presented here can be useful in a wide variety of contexts, ranging from weak interactions to electronic excitations to coordination chemistry. In particular, we discuss here how the scheme can be used for the characterization of the donation and back-donation components of metal−ligand bonds, in combination with the natural orbitals for chemical valence (NOCV) theory. In doing so, we discuss the interesting relationship between the proposed parameters and the corresponding NOCV eigenvalues, commonly used as a measure of the electron charge displacement associated with a given bonding contribution. As a prototype case study, we investigate the bond between a N-heterocyclic carbene and different metallic fragments. Finally, we show that our approach can be used in combination with the energy decomposition of the extended transition state method, providing an estimate of both charge transfer and polarization contributions to the interaction energy.

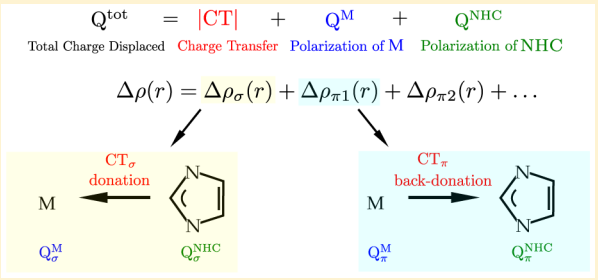

1. INTRODUCTION

Modern quantum chemistry methods have provided direct and accurate access to a wide range of molecular properties of interest for chemists, such as geometries, bond energies, and electron densities. At the same time, in order for our understanding of the chemical processes to evolve alongside with the increasing amount of data at our disposal, it has been necessary to develop models and interpretative frameworks by which to analyze the properties of molecules as well as their bonding and modes of interaction.[1] To this end, energy decomposition analysis (EDA) methods have proved to be extremely useful as they provide a quantification of the important components of the chemical interaction. The most popular of these methods are the symmetry adapted perturbation theory (SAPT),[2,3] extensively used in the context of weak interacting systems, and Morokuma-like EDA[4,5] such as the ALMO-EDA method of Head-Gordon[6] or the extended transition state (ETS) method of Ziegler.[7−9] This latter, implemented in combination with the natural orbitals for chemical valence (NOCV) theory,[9,10] finds widespread applications in the context of coordination chemistry. A second group of bond description schemes are based on the analysis of the electron density. Among these, we mention the natural bond orbitals (NBO) method,[11,12] atoms in molecules (AIM) theory,[13] electron localization function (ELF),[14] and charge decomposition analysis (CDA) developed by Dapprich and Frenking.[15]

We have proposed a simple yet powerful approach for analyzing a chemical bond in terms of the electron density rearrangement occurring upon formation of an adduct from two constituting fragments. Our approach relies on the charge displacement (CD) function,[16] measuring the electron charge displacement along a chosen axis occurring upon chemical bond formation. This method has been successfully used for quantifying the charge transfer (CT) component of the interaction in weakly interacting adducts[17−20] and more recently in the characterization of electronic transitions.[21] Above all, the CD scheme has been extremely successful in the study of the coordination bond. For systems of suitable symmetry, the CD function can be decomposed according to the irreducible representations of the point group to which the molecule belongs,[22,23] providing a clear-cut, quantitative picture of the donation and back-donation components of the Dewar−Chatt−Duncanson (DCD) model.[24,25] This has been very useful for the rationalization of spectroscopic data related to the σ acceptor or π donor properties of ligands and metallic fragments, permitting us to establish simple relationships between the DCD bonding components and experimental

Received: December 9, 2015
Published: January 29, 2016

DOI: 10.1021/acs.jctc.5b01166
J. Chem. Theory Comput. 2016, 12, 1236−1244

observables.[23,26−29] A recent development has permitted us to separate donation and back-donation also in the CD function of nonsymmetric systems by combining the CD scheme with the NOCV approach[30] (NOCV-CD).

In the present contribution, we propose a useful development of the CD methodology, which can be gainfully used in all of the above-mentioned situations. In Section 2.1, we introduce new simple descriptors, condensing the information on charge reorganization upon bond formation to few parameters. Having defined the general expression of these indexes, we show in Section 2.2 how these descriptors can be extracted by means of a proper decomposition of the CD function into its "accumulation" and "depletion" components, allowing for a thorough description of interactions in terms of few "charge displacement parameters". In Section 2.3, we combine this approach with the above-mentioned NOCV-CD scheme, thus extending our analysis to the characterization of the donation and back-donation components of coordination chemistry. In doing so, we discuss the relationship between the NOCV eigenvalues, commonly used as a measure of the electron charge displacement associated with a given bonding contribution[31] and the proposed descriptors. The charge displacement parameters here defined promise to be very useful for the study of the charge transfer character of electronic transitions, where the development of new density based indexes is becoming a very active field of research.[32−37]

In Section 3, as prototype study cases, we analyze the interaction between different transition metals and a simple N-heterocyclic carbene (NHC), whose characterization in terms of DCD bonding components has been the subject of numerous experimental[38−45] and theoretical[46−53] studies. In particular, our descriptors are applied to the study of the ligand effect on the Au−NHC bond in $[Au(NHC)]^+$, $[(CO)Au(NHC)]^+$, and $[(Cl)Au(NHC)]$ and of the metal effect on the M−NHC bond in a series of bis(carbene) complexes of formula $[M(NHC)_2]^{+/0}$, with M = Ni(0), Pd(0), Pt(0), Cu(I), Ag(I), and Au(I). Finally, in Section 3.3, we combine our approach with the already mentioned NOCV-ETS scheme, showing how these methods can merge synergically to provide new and quantitative information on the charge transfer and polarization contribution to the interaction energy.

2. THEORY AND COMPUTATIONAL DETAILS

2.1. Definition of Q^{tot}, Q^A, Q^B, and CT parameters. Our approach is based on the analysis of the electron density rearrangement $\Delta\rho(r)$ [where $r = (x, y, z)$ is the radius vector], defined as the difference between the electron density of a molecule AB and that of its two constituting fragments, A and B, placed in the positions they occupy in the adduct. In calculating $\Delta\rho$, one may simply take as initial density the sum of the densities of the isolated, noninteracting, A and B fragments or the density corresponding to a properly antisymmetrized product of the A and B wave functions (the so-called *promolecule*). These two differ for a small antisymmetrization term (see ref 30), and the following presentation applies identically to either choice.

$\Delta\rho(r)$ typically shows alternating regions of charge accumulation (positive values) and depletion (negative values) that define two different positive functions, $\Delta\rho^+$ and $\Delta\rho^-$, each equal to the magnitude of the appropriate portion, i.e.,

$$\Delta\rho^{\pm}(r) = \max[\pm\Delta\rho(r), 0] \tag{1}$$

so that

$$\Delta\rho = \Delta\rho^+ - \Delta\rho^- \tag{2}$$

We now define a quantity Q^{tot} as the integral of $\Delta\rho^+$ (or $\Delta\rho^-$) over the whole space

$$Q^{tot} = \int_{-\infty}^{\infty} \Delta\rho^+(r)\mathrm{d}r = \int_{-\infty}^{\infty} \Delta\rho^-(r)\mathrm{d}r \tag{3}$$

This measures the total net charge displacement accompanying bond formation. An analogous parameter has been introduced by Adamo et al. for studying the density variation associated with the excitation from the ground to exited states.[32,34]

By partitioning the space into two arbitrary regions, each associated with one of the interacting fragments, it is possible to define the charge transfer accompanying bond formation as

$$\mathrm{CT} = \int_A \Delta\rho(r)\mathrm{d}r = -\int_B \Delta\rho(r)\mathrm{d}r \tag{4}$$

or, in terms of $\Delta\rho^+$ and $\Delta\rho^-$

$$\mathrm{CT} = \int_A \Delta\rho^+(r)\mathrm{d}r - \int_A \Delta\rho^-(r)\mathrm{d}r = -\int_B \Delta\rho^+(r)\mathrm{d}r + \int_B \Delta\rho^-(r)\mathrm{d}r \tag{5}$$

where $\int_A$ and $\int_B$ are the integrals over the two fragment regions just mentioned. In these definitions, a positive CT value corresponds to charge transfer in the A ← B direction, while a negative value denotes charge transfer in the opposite direction.

The relationship between Q^{tot} and CT is interesting and is readily made explicit by combining eqs 3 and 5

$$\begin{aligned} Q^{tot} &= \int_A \Delta\rho^+(r)\mathrm{d}r + \int_B \Delta\rho^+(r)\mathrm{d}r \\ &= \mathrm{CT} + \int_A \Delta\rho^-(r)\mathrm{d}r + \int_B \Delta\rho^+(r)\mathrm{d}r \\ &= -\mathrm{CT} + \int_A \Delta\rho^+(r)\mathrm{d}r + \int_B \Delta\rho^-(r)\mathrm{d}r \end{aligned} \tag{6}$$

which, in view of the fact that when CT > 0, fragment B is the donor species (DON) and fragment A is the acceptor species (ACC), while when CT < 0, their role is swapped, can be concisely written as

$$Q^{tot} = |\mathrm{CT}| + Q^{DON} + Q^{ACC} \tag{7}$$

defining the fragment charges

$$Q^{DON} = \int_{DON} \Delta\rho^+(r)dr \qquad Q^{ACC} = \int_{ACC} \Delta\rho^-(r)dr \tag{8}$$

Of course, if CT = 0, there is no donor/acceptor species, and the integrals of $\Delta\rho^+$ and $\Delta\rho^-$ over a fragment space are equal. Alternatively, without reference to the fragment donor/acceptor role, we can put

$$Q^{tot} = |\mathrm{CT}| + Q^A + Q^B \tag{9}$$

where

DOI: 10.1021/acs.jctc.5b01166
J. Chem. Theory Comput. 2016, 12, 1236−1244

$$Q^{A} = \begin{cases} \int_{A} \Delta\rho^{-}(r)\mathrm{d}r & \text{if CT} > 0 \\ \int_{A} \Delta\rho^{+}(r)\mathrm{d}r & \text{if CT} < 0 \end{cases} \tag{10}$$

$$Q^{B} = \begin{cases} \int_{B} \Delta\rho^{+}(r)\mathrm{d}r & \text{if CT} > 0 \\ \int_{B} \Delta\rho^{-}(r)\mathrm{d}r & \text{if CT} < 0 \end{cases} \tag{11}$$

The charges Q^{ACC} and Q^{DON}, or Q^{A} and Q^{B}, quantify the electron displacement that bond formation causes within each fragment excluding charge transfer, thus including the charge rearrangement due to polarization. Clearly, since $\Delta\rho^{+}$ and $\Delta\rho^{-}$ are non-negative functions, and it follows that $|CT| \leq Q^{tot}$ and that $|CT| = Q^{tot}$ if and only if charge depletion (accumulation) areas are localized exclusively within the donor (acceptor) fragment.

2.2. Q^{tot}, Q^{A}, Q^{B}, and CT Parameters in the CD Framework. In this section, we show how the parameters just defined can be extracted from a suitable decomposition of the charge displacement (CD) function,[16] defined as

$$\Delta q(z) = \int_{-\infty}^{z}\int_{-\infty}^{\infty}\int_{-\infty}^{\infty} \Delta\rho(x, y, z')\mathrm{d}x\mathrm{d}y\mathrm{d}z' \tag{12}$$

This function gives, at a given point z along a chosen axis (typically connecting two fragments), the amount of electron charge that is transferred upon bond formation across a plane perpendicular to the axis at z in the direction of decreasing z. This function can be partitioned using eq 1 into "depletion" (Δq^{-}) and "accumulation" (Δq^{+}) components

$$\Delta q(z) = \Delta q^{+}(z) - \Delta q^{-}(z) \tag{13}$$

where

$$\Delta q^{+}(z) = \int_{-\infty}^{z}\int_{-\infty}^{\infty}\int_{-\infty}^{\infty} \Delta\rho^{+}(x, y, z')\mathrm{d}x\mathrm{d}y\mathrm{d}z' \tag{14}$$

$$\Delta q^{-}(z) = \int_{-\infty}^{z}\int_{-\infty}^{\infty}\int_{-\infty}^{\infty} \Delta\rho^{-}(x, y, z')\mathrm{d}x\mathrm{d}y\mathrm{d}z' \tag{15}$$

so that

$$Q^{tot} = \lim_{z\to+\infty} \Delta q^{+}(z) = \lim_{z\to+\infty} \Delta q^{-}(z) \tag{16}$$

By defining a suitable boundary between the fragments (z_{bound}), whereby fragment A is located at $z < z_{bound}$ and fragment B at $z > z_{bound}$, these functions permit a simple quantification of the parameters of eq 9

$$CT = \Delta q(z_{bound}) \tag{17}$$

$$Q^{A} = \begin{cases} \Delta q^{-}(z_{bound}) & \text{if CT} > 0 \\ \Delta q^{+}(z_{bound}) & \text{if CT} < 0 \end{cases} \tag{18}$$

$$Q^{B} = \begin{cases} Q^{tot} - \Delta q^{+}(z_{bound}) & \text{if CT} > 0 \\ Q^{tot} - \Delta q^{-}(z_{bound}) & \text{if CT} < 0 \end{cases} \tag{19}$$

As is true in general, these quantities depend on how space is partitioned to define the two "fragments" in the complex. In the present approach, this is accomplished by the single parameter z_{bound} and presupposes that the two fragments may be meaningfully separated by a single plane along a well-defined interaction axis. This is true of many systems we have successfully investigated with the CD approach[19,29,54] and of the systems discussed in the present work, but there may be interesting cases, for example, complexes where a metal is bound to a polydentate ligand, where this simple scheme may need revision or further elaboration. In general, any definition of charge-transfer related quantities suffers from some arbitrariness and limitation. The CD function has the clear advantage of providing a simple yet complete picture of charge displacement across the whole chemical system and thus permits an immediate useful assessment of the sensitivity of these parameters to variations in the fragment boundary in any specific application. We shall come back to this point in Section 3. Our standard choice of z_{bound} is the so-called "isodensity boundary",[16] namely, the z point where equal-valued isodensity surfaces of the isolated fragments become tangent.

2.3. Q^{tot}, Q^{A}, Q^{B} and CT Parameters in the NOCV-CD Framework. The charge displacement parameters we have introduced may be easily split into partial contributions that reflect actual charge flows of different entity and direction, thus casting light into the nature and composition of chemical interactions. One of the most well-established and powerful examples of such decomposition is the Dewar−Chatt−Duncanson donation/back-donation model of the coordination bond,[24,25] which we shall analyze in detail in the next section. To achieve this decomposition, we make use of the natural orbital for chemical valence theory[10] in combination with the CD analysis (NOCV-CD[30]). In this approach, we take $\Delta\rho$ as defined with reference to the promolecule, which can be brought into diagonal form in terms of NOCVs, which are the eigenfunctions φ_k of the "valence operator"[55−57]

$$\hat{V} = \sum_{i} (|\psi_i^{(AB)}\rangle\langle\psi_i^{(AB)}| - |\psi_i^{0}\rangle\langle\psi_i^{0}|) \tag{20}$$

where ψ_i^{0} is the set of the occupied Kohn−Sham orbitals of fragments A and B, mutually orthonormalized, and $\psi_i^{(AB)}$ is the set of occupied orbitals of the adduct.

The NOCVs can be grouped in pairs of complementary orbitals (φ_k, φ_{-k}) corresponding to eigenvalues with same absolute value but opposite sign[58]

$$\hat{V}\varphi_{\pm k} = \pm\nu_k\varphi_{\pm k} (\nu_k > 0) \tag{21}$$

where k numbers the NOCV pairs (we assume in descending order of ν_k). In terms of NOCV pairs, $\Delta\rho$ reads

$$\Delta\rho = \sum_{k} \nu_k(|\varphi_k|^2 - |\varphi_{-k}|^2) = \sum_{k} \Delta\rho_k \tag{22}$$

The CD function (eq 12), as well as its accumulation (eq 14) and depletion (eq 15) components can be defined for each $\Delta\rho_k$ contribution, thus permitting us to define Q^{tot}, CT, Q^{A}, and Q^{B} for each NOCV pair, whereby

$$Q_k^{tot} = |CT_k| + Q_k^{A} + Q_k^{B} \tag{23}$$

It needs perhaps be made explicit that these quantities separately characterize individual components of the density difference, which add and subtract variously in forming the total; therefore, they do not add up to the corresponding quantities that characterize the net $\Delta\rho$ of eqs 6−11. More precisely, the positive and negative portions of different $\Delta\rho_k$ components interfere with each other, so that $\Delta\rho^{\pm} \neq \sum_k \Delta\rho_k^{\pm}$. On the other hand, the CT_k values, which depend on the

DOI: 10.1021/acs.jctc.5b01166
J. Chem. Theory Comput. 2016, 12, 1236−1244

additive $\Delta\rho_k$ functions and not on their positive or negative parts, do add up to the net charge transfer.

According to eq 22, an eigenvalue ν_k may be seen as the fraction of electron transferred from the φ_{-k} (donor) to the φ_k (acceptor) orbital. It is therefore interesting to discuss in more detail how the charge transfer between these two orbitals is reflected into the actual spatial charge rearrangement taking place. To do that, we recall the definition of $\Delta\rho_k^+$

$$\Delta\rho_k^+(r) = \begin{cases} \nu_k(|\varphi_k|^2 - |\varphi_{-k}|^2) & \text{if } \Delta\rho_k(r) > 0 \\ 0 & \text{if } \Delta\rho_k(r) \le 0 \end{cases} \tag{24}$$

from which Q_k^{tot} can be written as

$$\begin{aligned} Q_k^{tot} &= \nu_k \int_{\Delta\rho_k>0} (|\varphi_k(r)|^2 - |\varphi_{-k}(r)|^2)\mathrm{d}r \\ &= \nu_k \int_{-\infty}^{\infty} |\varphi_k(r)|^2\mathrm{d}r - \nu_k \int_{\Delta\rho_k<0} |\varphi_k(r)|^2\mathrm{d}r \\ &\quad - \nu_k \int_{\Delta\rho_k>0} |\varphi_{-k}(r)|^2\mathrm{d}r \\ &= \nu_k\left(1 - \int_{\Delta\rho_k<0} |\varphi_k(r)|^2\mathrm{d}r - \int_{\Delta\rho_k>0} |\varphi_{-k}(r)|^2\mathrm{d}r\right) \end{aligned} \tag{25}$$

where, $\int_{\Delta\rho_k>0}$ ($\int_{\Delta\rho_k<0}$) is the integral over the region in which $\Delta\rho_k$ assumes positive (negative) values. Equation 25 shows that $Q_k^{tot} \le \nu_k$, i.e., ν_k is an upper bound for the actual charge rearrangement taking place, and $Q_k^{tot} = \nu_k$ only if $|\varphi_k|$ and $|\varphi_{-k}|$ are non-zero in different regions ($|\varphi_k(r)||\varphi_{-k}(r)| = 0$ everywhere), which means that $\Delta\rho_k^+ = |\varphi_k|^2$ and $\Delta\rho^-{}_k = |\varphi_{-k}|^2$. Similarly, from the definition of CT follows

$$\begin{aligned} \mathrm{CT}_k &= \int_A \Delta\rho_k(r)\mathrm{d}r = \int_A \nu_k(|\varphi_k(r)|^2 - |\varphi_{-k}(r)|^2)\mathrm{d}r \\ &= \nu_k\left(1 - \int_A |\varphi_{-k}(r)|^2\mathrm{d}r - \int_B |\varphi_k(r)|^2\mathrm{d}r\right) \end{aligned} \tag{26}$$

which explicitly shows that $\mathrm{CT}_k \le \nu_k$, with equality holding only if the donor and the acceptor orbitals are entirely localized within different fragments (note that in this case $\nu_k = Q_k^{tot} = |\mathrm{CT}_k|$).

2.4. Computational Details. Geometries and electron densities were calculated with the Amsterdam density functional (ADF) package[59−61] by means of density functional theory (DFT) using the Becke's exchange functional[62] plus the Lee−Yang−Parr correlation functional[63] (BLYP). All electron triple-ζ basis sets with two polarization functions (TZ2P) and a small frozen core has been used for all atoms. Relativistic effects were included by means of the zeroth-order regular approximation (ZORA) Hamiltonian.[64−66] Electron densities were mapped on a regular grid of points using the densf auxiliary program provided by the ADF package. Charge displacement functions and all the density-based parameters were computed using numerical integration procedure with an internally developed software.

3. APPLICATIONS

3.1. Ligand Effect in Gold(I) Complexes. As a first illustrative example, we study how the charge displacement parameters can be used to characterize the coordination bond between a simple N-heterocyclic carbene and a gold(I)−ligand fragment in linear complexes of formula [(L)Au(NHC)], where NHC is imidazol-2-ylidene. These type of systems are receiving increasing attention in homogeneous gold(I) catalysis,[67−70] where the different π acidity of N-heterocyclic carbenes in the bond with Au(I) may, in some cases, determine the mechanism of gold-catalyzed processes.[43]

We analyze the charge flows associated with the formation of the bond between gold and NHC in three gold(I) complexes, namely, $[(CO)Au(NHC)]^+$, [(Cl)Au(NHC)], and the ligand-free $[Au(NHC)]^+$. Of course, we consider as binding fragments in each case NHC and the remaining gold−ligand moiety and as integration axis the one joining the gold atom and the cabenic carbon. These systems differ for the ligand in trans with respect to NHC, which modulates the π component of the Au−NHC interaction, as we previously[52] demonstrated by means of the symmetry partitioning of the electron density difference.[22,23]

As reported in ref 52, three main charge transfer components constitute the Au−C (of NHC) bond, namely the Au ← C σ donation from the lone pair on the carbenic carbon to the empty s orbitals of gold(I), the out of plane Au → C π back-donation to the empty p orbital perpendicular to the carbene ring (π_1), and another minor in-plane Au → C π back-donation component (π_2). The NOCV decomposition singles out these main bond components as three density contributions $\Delta\rho_k$, whose 3D contour plots are shown in Figure 1. The detailed

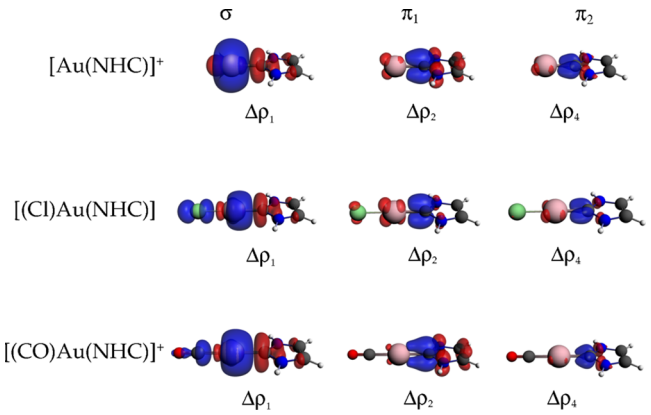

Figure 1. $\Delta\rho_k$ components (isosurface values: ± 0.002 e/a.u.^{3}) for the Au−C chemical bond formation in $[Au(NHC)]^+$ (first row), [(Cl)Au(NHC)] (second row), and $[(CO)Au(NHC)]^+$ (third row) grouped (columns) according to their σ, π_1, and π_2 character (see text for details). Red surfaces identify charge depletion areas; blue surfaces identify charge accumulation areas.

quantitative characterization of the charge transfer and polarization components that the analysis outlined in the previous section can provide is clearly displayed in Figure 2 for the two largest NOCV contributions, $\Delta\rho_1$ and $\Delta\rho_2$, in the $[Au(NHC)]^+$ case. Let us start from $\Delta\rho_1$ (upper panel of Figure 2), which correlates with the Au ← C σ donation component. The corresponding CD function $\Delta q_1(z)$ (black solid line in the figure) is positive everywhere in the Au−C bonding region, indicating that charge flows in the direction from NHC to the gold fragment. As discussed in the previous section, the isodensity boundary point (z_{bound}) on the curve marked as CT_1 (0.48 e) can be usefully taken as a measure of the corresponding σ donation (the vertical gray band in the figure is centered about this point). The solid blue and red curves correspond to the accumulation Δq_1^+ and depletion Δq_1^-

DOI: 10.1021/acs.jctc.5b01166
J. Chem. Theory Comput. 2016, 12, 1236−1244

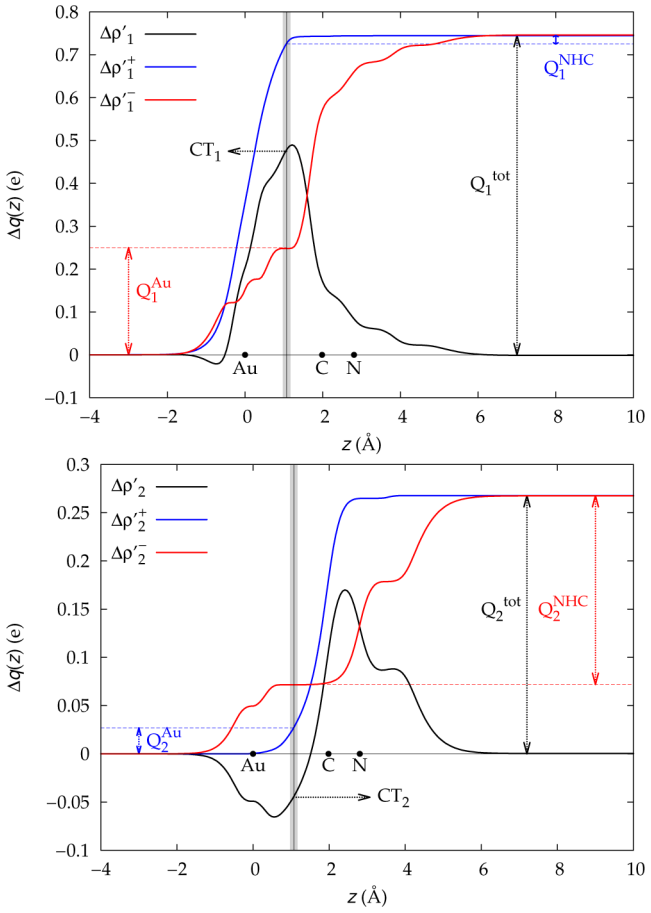

Figure 2. Solid black lines are CD functions associated with $\Delta\rho_k$ ($k = 1$ upper panel, $k = 2$ lower panel) components for the Au−C bond in $[Au(NHC)]^+$. Their constituting accumulation (solid blue) and depletion (solid red) components as well as the CT_k, Q_k^{tot}, Q_k^{NHC}, and Q_k^{Au} parameters defined in Section 2.2 are also reported. Black dots mark the z coordinate of Au and carbenic carbon atoms. The vertical gray band is centered about the isodensity boundary. See text for further details.

components (eqs 14 and 15), respectively, of the CD function. According to the previous discussion, the unique asymptotic value of these functions gives the total charge displaced in the NOCV pair ($Q_1^{tot} = 0.74$ e). As expected (eq 23), this is larger than CT_1 by a quantity corresponding to the internal charge rearrangement of the two fragments (pertaining to the NOCV pair at hand). As the figure shows, for the left fragment (gold in this case), this internal charge rearrangement is equal to the value at z_{bound} of the depletion or of the accumulation curve depending on whether the fragment is the acceptor (as gold is for the σ donation component) or the donor one. For the right fragment (NHC), the charge rearrangement is the difference between Q^{tot} and the value at z_{bound} of the complementary accumulation or depletion curve. What we see in the present case of the Au ← NHC donation is that almost the entire internal charge rearrangement (equal to about half the CT) is confined to gold. This is evidenced by the large drop in electron density on the far side of the gold atom opposite to the carbene (positive slope of the depletion curve) and is a consequence of the formation of a strong gold−carbene σ bond, which in turn causes a rehybrization of the gold orbitals.[16] By contrast, Q_1^{NHC} is very small (0.02 e), as charge accumulation takes place almost entirely within the acceptor Au^+ fragment, where the accumulation blue curve nearly reaches its asymptotic value and remains almost constant thereafter.

In the lower panel of Figure 2, the same analysis is displayed for the $\Delta\rho_2$ component of the Au−C bond, which correlates with the Au → C π back-donation. The black curve is now negative in the Au−C bonding region, which indicates a charge flow going in the direction from gold to the NHC fragment. In this case, the CT_2 isodensity boundary value is −0.04 e (the sign indicates the direction of the flow; see eq 12), quantifying a very small back-donation compared to the σ donation component above. However, the total charge rearrangement (Q_2^{tot}) is again more than 0.2 e larger than $|CT_2|$ and also in this case almost entirely due to the rearrangement taking place within the acceptor fragment (NHC). This measures the polarization of the π electrons of the carbene upon interaction with the positively charged Au^+ fragments, which in turn contributes, together with the Au → NHC back-donation, to the significant charge accumulation in the region of the formally empty p orbital of the carbenic carbon atom. In an orbital picture, we are thus able to quantify how the back-donation (CT_2) and the polarization of the NHC moiety (Q_2^{NHC}) compete for populating the formally empty p orbital of the carbenic carbon upon formation of the gold−carbon bond. More generally, the detailed characterization of the effects measured by the parameters introduced here can be very useful to better understand the nature of coordination bonds and for the rationalization of experimental observables related to the magnitude of the DCD bonding components.[23] As to the robustness of these charge displacement parameters, we underline again that the CD functions themselves provide a very good assessment tool. In the present case, Figure 2 clearly shows that the parameters just discussed are only weakly dependent on any meaningful variation of the boundary chosen for separating the fragments; by changing the position of the boundary within the gray band (the width of which is 10% of the Au−C bond length), the polarization and charge transfer parameters change slightly, whereas the overall charge displaced is by definition independent on how the space is partitioned.

In the remainder of this section, we use the computed NOCV-CD parameters for comparing the Au−C bond features of the ligand-free $[Au(NHC)]^+$ system with those of [(CO)-Au(NHC)]$^+$ and [(Cl)Au(NHC)]. The parameters for the relevant $\Delta\rho_k$ component are displayed in Table 1, together with the corresponding ν_k eigenvalues. A graphical version of these data is presented in Figure 3, where each Q_k^{tot} is decomposed into the charge transfer component ($|CT_k|$, red bar), polarization of the NHC moiety (Q_k^{NHC}, blue bar), and polarization of the metallic fragment (Q_k^{Au}, light blue bar). By looking at the figure, the first eye-catching feature is that the σ donation contribution to the overall electron density change involves a larger overall charge displacement than the π_1 and π_2 components for all systems. This is especially true of the ligand-free system, with its particularly large Au^+ rearrangement. The other two complexes show a decomposition pattern of $\Delta\rho_1$ very similar to each other. This similarity is not especially surprising, as the relative invariance of the Au−C σ donation component of linear gold(I) complexes to changes in the ancillary ligand has already been evidenced both with NHC[52] and with other substrates.[26] Turning to the π_1 component of the bond, it is somewhat counterintuitive to find that the total charge displaced is smallest in the case of the Cl^- ligand, which is a strong π donor and is expected to enhance π back-donation toward the NHC. But eq 9 or eq 23

DOI: 10.1021/acs.jctc.5b01166
J. Chem. Theory Comput. 2016, 12, 1236−1244

Table 1. Q_k^{tot} Parameters and Their Decomposition into Charge Transfer (CT_k) and Polarization (Q_k^{NHC} and Q_k^{Au}) for σ, π_1, and π_2 Components of the Au−C Interaction[a]

	ligand	ν_k (e)	Q_k^{tot} (e)	CT_k (e)	Q_k^{NHC} (e)	Q_k^{LAu} (e)
σ comp.						
(k = 1)	none	0.95	0.74	0.48	0.02	0.25
(k = 1)	Cl^-	0.56	0.43	0.31	0.04	0.08
(k = 1)	CO	0.59	0.45	0.34	0.05	0.06
π_1 comp.						
(k = 2)	none	0.35	0.27	−0.04	0.20	0.03
(k = 2)	Cl^-	0.38	0.17	−0.11	0.05	0.01
(k = 2)	CO	0.32	0.25	0.00	0.21	0.04
π_2 comp.						
(k = 4)	none	0.16	0.10	−0.03	0.06	0.01
(k = 4)	Cl^-	0.18	0.08	−0.04	0.03	0.01
(k = 4)	CO	0.13	0.08	−0.02	0.05	0.01

[a]Corresponding NOCV eigenvalues ν_k are also reported for comparison.

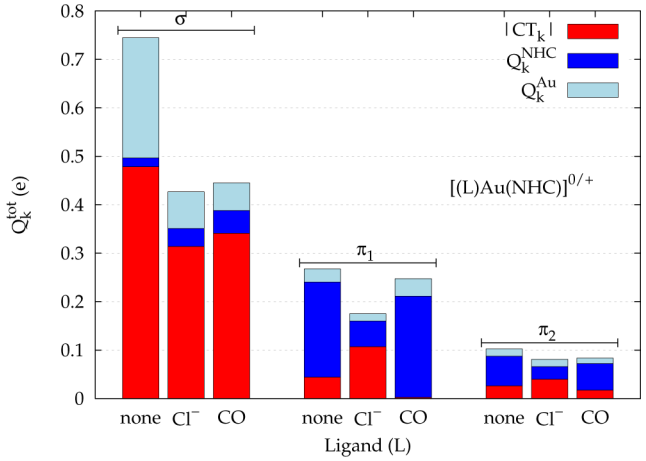

Figure 3. Q_k^{tot} associated with σ, π_1, and π_2 components of the Au−NHC interaction and their decomposition according to eq 9.

make it clear that the total charge displaced results as the sum of charge transfer and polarization, and therefore, there is in principle no reason why it should directly correlate with either component since these are controlled by different factors. In particular, we see here that the net back-donation is indeed largest for the Cl^- species, but NHC polarization is instead comparatively much larger in the charged species $[Au(NHC)]^+$ and $[(CO)Au(NHC)]^+$ than in the neutral $[(Cl)Au(NHC)]$ because the positively charged fragments exert a stronger electric field on the NHC moiety. As a result, the total charge displaced is smallest in the latter system (despite this showing the largest back-donation component) and largest in the case of the naked Au^+ fragment, which gives a non-negligible back-donation and at the same time polarizes the NHC ligand significantly.

3.2. Metal Effect in Bis(carbene) Complexes. The same approach used above can be applied to study and compare the behavior of different metals in coordinating a ligand. By way of example, we show here the results for the M−NHC bond in a series of homoleptic compounds of formula $[M(NHC)_2]^{+/0}$, Ni(0), Pd(0), Pt(0), Cu(I), Ag(I), and Au(I) (fragments are NHC and remaining metal−NHC moiety). These are slightly simplified models of experimentally characterized compounds, some of which have been proposed to be key intermediates of several organic transformations.[71−75] The main components of the interaction are those already discussed (σ, π_1, and π_2), and the qualitative shape of the contour plots of each component is the same for all the systems. We shall therefore just focus on the quantitative insight provided by the Q_k^{tot} decomposition, reported in Table 2 and Figure 4.

Table 2. Q_k^{tot} Parameters and Their Decomposition into Charge Transfer (CT_k) and Polarization (Q_k^{NHC} and Q_k^{Au}) for σ, π_1, and π_2 Components of the M−NHC Interaction in $M(NHC)_2$ Complexes[a]

DCD comp.	metal	ν_k (e)	Q_k^{tot} (e)	CT_k (e)	Q_k^{NHC} (e)	Q_k^{M} (e)
σ comp.						
(k = 2)	Ni(0)	0.37	0.28	0.18	0.06	0.04
(k = 2)	Pd(0)	0.38	0.28	0.17	0.04	0.06
(k = 2)	Pt(0)	0.47	0.32	0.24	0.05	0.02
(k = 1)	Cu(I)	0.41	0.29	0.22	0.06	0.02
(k = 1)	Ag(I)	0.45	0.34	0.23	0.04	0.06
(k = 1)	Au(I)	0.55	0.40	0.31	0.05	0.05
π_1 comp.						
(k = 1)	Ni(0)	0.58	0.25	−0.23	0.00	0.01
(k = 1)	Pd(0)	0.40	0.13	−0.13	0.00	0.00
(k = 1)	Pt(0)	0.48	0.18	−0.18	0.00	0.01
(k = 2)	Cu(I)	0.28	0.19	−0.04	0.13	0.02
(k = 2)	Ag(I)	0.23	0.17	−0.02	0.13	0.02
(k = 2)	Au(I)	0.28	0.20	−0.04	0.14	0.02
π_2 comp.						
(k = 3)	Ni(0)	0.19	0.06	−0.04	0.01	0.00
(k = 4)	Pd(0)	0.16	0.05	−0.03	0.01	0.00
(k = 3)	Pt(0)	0.20	0.07	−0.05	0.01	0.01
(k = 4)	Cu(I)	0.12	0.07	−0.02	0.03	0.01
(k = 4)	Ag(I)	0.11	0.06	−0.01	0.03	0.01
(k = 4)	Au(I)	0.16	0.07	−0.03	0.02	0.02

[a]Corresponding NOCV eigenvalues ν_k are also reported for comparison.

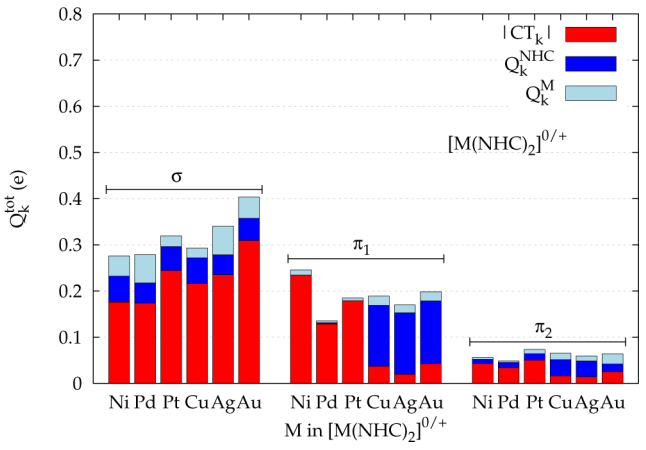

Figure 4. Q_k^{tot} associated with σ, π_1, and π_2 components of the M−NHC interaction and their decomposition according to eq 9.

As before, the σ component of the interaction is generally accompanied by the largest amount of charge displaced, but it is immediately evident that the nickel complex is somewhat exceptional in this respect, in that the σ and π_1 components show similar Q_k^{tot} values. As expected, changing the metal affects the M−NHC bonding features in significant ways. The total charge displaced ranges from 0.28 e for the Ni and Pd

DOI: 10.1021/acs.jctc.5b01166
J. Chem. Theory Comput. 2016, 12, 1236−1244

complexes to 0.40 e for the Au one, and the σ donation almost doubles from 0.17 e for Pd to 0.31 e for Au. With the noted exception of Ni, where it is largest (0.25 e), and of Pd, where it is smallest (0.13 e), the π_1 displacement is quite constant, but the actual back-donation and NHC polarization components vary very significantly between the neutral and the charged species. For the zero-valent metals, almost the entire Q_k^{tot} is due to back-donation, while the charged coinage metals, although back-donating much less, strongly polarize the NHC ligand. The net result of this larger sensitivity of the π density change to the charge of the metal fragment is that, once again contrary to the σ density, total charge displaced and charge transfer do not follow the same trend. We note a greater value of π back-donation in the Ni complex compared with that of Pd. This is consistent with the trend in stretching frequency observed of the respective carbonyl compounds[76] and in accordance with the low metal atom ionization potential.

3.3. Charge Transfer and Polarization Contribution to Energy. As a last aspect of our analysis, we propose a preliminary discussion of how it can usefully complement energy decomposition models and help to estimate the CT and polarization contributions to the interaction energy for specific bonding components. To do this, we take advantage of the NOCV-ETS approach, which permits to separate contributions ΔE_k (associated with different $\Delta\rho_k$ values) of the interaction energy.[9] Let us focus in particular on the π_1 contribution of metal−carbon bonds, where we have seen that that both CT and polarization may contribute significantly and to a varying extent to the electron density rearrangement. As we have just discussed, the π_1 metal−NHC interaction is almost completely dominated by CT in the Ni, Pd, and Pt case. In particular, in the case of $[Pt(NHC)_2]$ ($|CT_k|$ = 0.179 e), where this dominance is actually largest, the corresponding NOCV-ETS π_1 energy is E_k = 15.5 kcal/mol, and we may safely take this to be entirely due to CT. If we make the assumption that the CT energy contribution is generally proportional to the actual charge transferred,[6,12,20] this yields a proportionality factor of 86.6 kcal/mol per electron transferred. It is reasonable to assume this factor to be roughly constant for interactions of a similar nature.[19] Indeed, the corresponding ratio for the Ni complex is 86.9 kcal/mol/e, and for the Pd complex (where CT_k is a slightly smaller fraction of Q_k^{tot}), it is 89.1 kcal/mol/e. These figures are also comfortably close to an estimate obtained by a simple charge delocalization model[19] and to what has been found by combining CD analysis with high-resolution crossed-beam experiments of weakly interacting adducts.[17] With these simple assumptions, and the data in Table 2, it is easy to estimate the CT and (by difference) the polarization contributions to the NOCV-ETS π_1 energy for the whole series of complexes studied here, as shown in Table 3. We leave a much more detailed discussion and verification of the suggestions presented here to future studies.

Table 3. Energy Contributions ΔE_k Associated with the π Component of the M−C Interaction[a]

	ΔE_k (π) (kcal/mol)	ΔE_k^{CT} (π)	ΔE_k^{Pol} (π)	$\frac{\Delta E_k^{CT}}{\Delta E_k}$%
$[Ni(NHC)_2]$	−20.4	−20.4	0.0	100
$[Pt(NHC)_2]$	−15.5	−15.5	0.0	100
$[Au(NHC)]^+$	−14.8	−3.8	−11.0	26
$[(CO)Au(NHC)]^+$	−11.7	−0.2	−11.5	2
$[Pd(NHC)_2]$	−11.4	−11.1	−0.3	97
[(Cl)Au(NHC)]	−11.1	−9.3	−1.8	84
$[Au(NHC)_2]^+$	−9.1	−3.7	−5.4	41
$[Cu(NHC)_2]^+$	−8.7	−3.2	−5.5	37
$[Ag(NHC)_2]^+$	−6.3	−1.7	−4.6	27

[a]Its decomposition into charge transfer (ΔE_k^{CT}) and polarization ΔE_k^{pol} contributions is also reported. See text for discussion.

4. CONCLUSIONS

We have studied electron density-based descriptors for the quantification of charge transfer and polarization effects associated with the formation of a chemical bond between two interacting fragments, which condense the information on the resulting charge reorganization into few useful parameters. These parameters quantify the total charge displaced upon bond formation and decompose it into a charge transfer component between the fragments and charge rearrangements taking place within the fragments. Having defined the general expression of these indexes, which are based on a suitable spatial definition of the fragments in the complex and the integration of the electron density difference accompanying bond formation, we showed how they can be simply calculated by taking advantage of the charge displacement scheme, which has already proved to be a powerful tool for studying charge reorganization processes in a wide range of chemical interactions. We then showed how, by taking advantage of the properties of the natural orbital for chemical valence (NOCV), the proposed tools can be usefully applied to analyze the charge rearrangements associated with different components of chemical bonds, such as the donation and back-donation components of metal−ligand coordination bonds. In this context, we have also discussed in detail the insightful relationship between NOCV eigenvalues and the proposed descriptors.

As a case study, we have applied our scheme to the interaction between a N-heterocyclic carbene (NHC) and different metallic fragments. This has permitted us to illustrate the use of the proposed charge displacement parameters and at the same time has provided useful information on the coordination bond. In the last part of the paper, we showed how our charge decomposition scheme, in combination with the well-established NOCV-ETS analysis, can be usefully applied for establishing the CT contribution to the interaction energy of the M−NHC bond. We believe the charge displacement parameters proposed here can thus be useful in a variety of circumstances to provide quantitative insights into the nature of chemical bonds and for the modeling of intermolecular interactions.

■ ASSOCIATED CONTENT

Ⓢ Supporting Information

The Supporting Information is available free of charge on the ACS Publications website at DOI: 10.1021/acs.jctc.5b01166.

DFT-optimized geometries for all the complexes studied. (ZIP)

■ AUTHOR INFORMATION

Corresponding Author

*E-mail: giovanni@thch.unipg.it.

Notes

The authors declare no competing financial interest.

DOI: 10.1021/acs.jctc.5b01166
J. Chem. Theory Comput. 2016, 12, 1236−1244

■ ACKNOWLEDGMENTS

This work has been supported by Ministero dell'Istruzione, Università e Ricerca (MIUR) through the FIRB *Futuro in Ricerca* project n. RBFR1022UQ.

■ REFERENCES

(1) Frenking, G., Shaik, S., Eds.; *The Chemical Bond: Fundamental Aspects of Chemical Bonding*; John Wiley & Sons, 2014.
(2) Rybak, S.; Jeziorski, B.; Szalewicz, K. *J. Chem. Phys.* **1991**, *95*, 6576−6601.
(3) Jeziorski, B.; Moszynski, R.; Szalewicz, K. *Chem. Rev.* **1994**, *94*, 1887−1930.
(4) Kitaura, K.; Morokuma, K. *Int. J. Quantum Chem.* **1976**, *10*, 325−340.
(5) Morokuma, K. *J. Chem. Phys.* **1971**, *55*, 1236−1244.
(6) Khaliullin, R. Z.; Cobar, E. A.; Lochan, R. C.; Bell, A. T.; Head-Gordon, M. *J. Phys. Chem. A* **2007**, *111*, 8753−8765.
(7) Ziegler, T.; Rauk, A. *Theor. Chim. Acta* **1977**, *46*, 1−10.
(8) Ziegler, T.; Rauk, A. *Inorg. Chem.* **1979**, *18*, 1558−1565.
(9) Mitoraj, M. P.; Michalak, A.; Ziegler, T. *J. Chem. Theory Comput.* **2009**, *5*, 962−975.
(10) Mitoraj, M.; Michalak, A. *J. Mol. Model.* **2007**, *13*, 347−355.
(11) Weinhold, F.; Landis, C. R. *Valency and Bonding: A Natural Bond Orbital Donor-Acceptor Perspective*; Cambridge University Press, 2005.
(12) Reed, A. E.; Curtiss, L. A.; Weinhold, F. *Chem. Rev.* **1988**, *88*, 899−926.
(13) Bader, R. F. W. *Encyclopedia of Computational Chemistry*; John Wiley & Sons, Ltd., 2002.
(14) Becke, A. D.; Edgecombe, K. E. *J. Chem. Phys.* **1990**, *92*, 5397−5403.
(15) Dapprich, S.; Frenking, G. *J. Phys. Chem.* **1995**, *99*, 9352−9362.
(16) Belpassi, L.; Infante, I.; Tarantelli, F.; Visscher, L. *J. Am. Chem. Soc.* **2008**, *130*, 1048−1060.
(17) Belpassi, L.; Reca, M. L.; Tarantelli, F.; Roncaratti, L. F.; Pirani, F.; Cappelletti, D.; Faure, A.; Scribano, Y. *J. Am. Chem. Soc.* **2010**, *132*, 13046−13058.
(18) Bistoni, G.; Belpassi, L.; Tarantelli, F.; Pirani, F.; Cappelletti, D. *J. Phys. Chem. A* **2011**, *115*, 14657−14666.
(19) Cappelletti, D.; Ronca, E.; Belpassi, L.; Tarantelli, F.; Pirani, F. *Acc. Chem. Res.* **2012**, *45*, 1571−1580.
(20) Ronca, E.; Belpassi, L.; Tarantelli, F. *ChemPhysChem* **2014**, *15*, 2682−2687.
(21) Ronca, E.; Pastore, M.; Belpassi, L.; De Angelis, F.; Angeli, C.; Cimiraglia, R.; Tarantelli, F. *J. Chem. Phys.* **2014**, *140*, 054110.
(22) Salvi, N.; Belpassi, L.; Tarantelli, F. *Chem. - Eur. J.* **2010**, *16*, 7231−7240.
(23) Bistoni, G.; Belpassi, L.; Tarantelli, F. *Angew. Chem., Int. Ed.* **2013**, *52*, 11599−11602.
(24) Dewar, M. *Bull. Soc. Chim. Fr.* **1951**, *18*, C71.
(25) Chatt, J.; Duncanson, L. *J. Chem. Soc.* **1953**, 2939−2947.
(26) Ciancaleoni, G.; Scafuri, N.; Bistoni, G.; Macchioni, A.; Tarantelli, F.; Zuccaccia, D.; Belpassi, L. *Inorg. Chem.* **2014**, *53*, 9907−9916.
(27) Ciancaleoni, G.; Biasiolo, L.; Bistoni, G.; Macchioni, A.; Tarantelli, F.; Zuccaccia, D.; Belpassi, L. *Chem. - Eur. J.* **2015**, *21*, 2467−2473.
(28) Azzopardi, K. M.; Bistoni, G.; Ciancaleoni, G.; Tarantelli, F.; Zuccaccia, D.; Belpassi, L. *Dalton Trans.* **2015**, *44*, 13999−14007.
(29) Bistoni, G.; Rampino, S.; Scafuri, N.; Ciancaleoni, G.; Zuccaccia, D.; Belpassi, L.; Tarantelli, F. *Chem. Sci.* **2016**, *7*, 1174−1184.
(30) Bistoni, G.; Rampino, S.; Tarantelli, F.; Belpassi, L. *J. Chem. Phys.* **2015**, *142*, 084112.
(31) Jerabek, P.; Roesky, H. W.; Bertrand, G.; Frenking, G. *J. Am. Chem. Soc.* **2014**, *136*, 17123−17135.
(32) Le Bahers, T.; Adamo, C.; Ciofini, I. *J. Chem. Theory Comput.* **2011**, *7*, 2498−2506.
(33) Savarese, M.; Netti, P. A.; Adamo, C.; Rega, N.; Ciofini, I. *J. Phys. Chem. B* **2013**, *117*, 16165−16173.
(34) Adamo, C.; Le Bahers, T.; Savarese, M.; Wilbraham, L.; García, G.; Fukuda, R.; Ehara, M.; Rega, N.; Ciofini, I. *Coord. Chem. Rev.* **2015**, *304*−*305*, 166−178.
(35) Etienne, T.; Assfeld, X.; Monari, A. *J. Chem. Theory Comput.* **2014**, *10*, 3906−3914.
(36) Etienne, T.; Assfeld, X.; Monari, A. *J. Chem. Theory Comput.* **2014**, *10*, 3896−3905.
(37) Etienne, T. *J. Chem. Theory Comput.* **2015**, *11*, 1692−1699.
(38) Hu, X.; Tang, Y.; Gantzel, P.; Meyer, K. *Organometallics* **2003**, *22*, 612−614.
(39) Mercs, L.; Labat, G.; Neels, A.; Ehlers, A.; Albrecht, M. *Organometallics* **2006**, *25*, 5648−5656.
(40) Sanderson, M. D.; Kamplain, J. W.; Bielawski, C. W. *J. Am. Chem. Soc.* **2006**, *128*, 16514−16515.
(41) Fantasia, S.; Petersen, J. L.; Jacobsen, H.; Cavallo, L.; Nolan, S. P. *Organometallics* **2007**, *26*, 5880−5889.
(42) Khramov, D. M.; Lynch, V. M.; Bielawski, C. W. *Organometallics* **2007**, *26*, 6042−6049.
(43) Alcarazo, M.; Stork, T.; Anoop, A.; Thiel, W.; Fürstner, A. *Angew. Chem., Int. Ed.* **2010**, *49*, 2542−2546.
(44) Back, O.; Henry-Ellinger, M.; Martin, C. D.; Martin, D.; Bertrand, G. *Angew. Chem., Int. Ed.* **2013**, *52*, 2939−2943.
(45) Vummaleti, S. V.; Nelson, D. J.; Poater, A.; Gómez-Suárez, A.; Cordes, D. B.; Slawin, A. M.; Nolan, S. P.; Cavallo, L. *Chem. Sci.* **2015**, *6*, 1895−1904.
(46) Jacobsen, H.; Correa, A.; Costabile, C.; Cavallo, L. *J. Organomet. Chem.* **2006**, *691*, 4350−4358.
(47) Tonner, R.; Heydenrych, G.; Frenking, G. *Chem. - Asian J.* **2007**, *2*, 1555−1567.
(48) Srebro, M.; Michalak, A. *Inorg. Chem.* **2009**, *48*, 5361−5369.
(49) Jacobsen, H.; Correa, A.; Poater, A.; Costabile, C.; Cavallo, L. *Coord. Chem. Rev.* **2009**, *253*, 687−703.
(50) Comas-Vives, A.; Harvey, J. N. *Eur. J. Inorg. Chem.* **2011**, *2011*, 5025−5035.
(51) Bernhammer, J. C.; Frison, G.; Huynh, H. V. *Chem. - Eur. J.* **2013**, *19*, 12892−12905.
(52) Marchione, D.; Belpassi, L.; Bistoni, G.; Macchioni, A.; Tarantelli, F.; Zuccaccia, D. *Organometallics* **2014**, *33*, 4200−4208.
(53) Rezabal, E.; Frison, G. *J. Comput. Chem.* **2015**, *36*, 564−572.
(54) Gaggioli, C. A.; Ciancaleoni, G.; Biasiolo, L.; Bistoni, G.; Zuccaccia, D.; Belpassi, L.; Belanzoni, P.; Tarantelli, F. *Chem. Commun.* **2015**, *51*, 5990−5993.
(55) Nalewajski, R. F.; Köster, A. M.; Jug, K. *Theor. Chim. Acta* **1993**, *85*, 463−484.
(56) Nalewajski, R. F.; Mrozek, J. *Int. J. Quantum Chem.* **1994**, *51*, 187−200.
(57) Nalewajski, R. F.; Mrozek, J.; Michalak, A. *Int. J. Quantum Chem.* **1997**, *61*, 589−601.
(58) Radoń, M. *Theor. Chem. Acc.* **2008**, *120*, 337−339.
(59) *ADF User's Guide*, Release 2012.01; SCM, Theoretical Chemistry, Vrije Universiteit: Amsterdam, The Netherlands, 2012.
(60) Fonseca Guerra, C.; Snijders, J. G.; te Velde, G.; Baerends, E. J. *Theor. Chem. Acc.* **1998**, *99*, 391−403.
(61) te Velde, G.; Bickelhaupt, F. M.; Baerends, E. J.; Fonseca Guerra, C.; van Gisbergen, S. J. A.; Snijders, J. G.; Ziegler, T. *J. Comput. Chem.* **2001**, *22*, 931−967.
(62) Becke, A. D. *Phys. Rev. A: At., Mol., Opt. Phys.* **1988**, *38*, 3098−3100.
(63) Lee, C.; Yang, W.; Parr, R. G. *Phys. Rev. B: Condens. Matter Mater. Phys.* **1988**, *37*, 785−789.
(64) van Lenthe, E.; Baerends, E. J.; Snijders, J. G. *J. Chem. Phys.* **1993**, *99*, 4597−4610.
(65) van Lenthe, E.; Baerends, E. J.; Snijders, J. G. *J. Chem. Phys.* **1994**, *101*, 9783−9792.
(66) van Lenthe, E.; Ehlers, A.; Baerends, E.-J. *J. Chem. Phys.* **1999**, *110*, 8943−8953.

DOI: 10.1021/acs.jctc.5b01166
J. Chem. Theory Comput. 2016, 12, 1236−1244

(67) Hashmi, A. S. K.; Hutchings, G. J. *Angew. Chem., Int. Ed.* **2006**, *45*, 7896−7936.
(68) Gorin, D. J.; Sherry, B. D.; Toste, F. D. *Chem. Rev.* **2008**, *108*, 3351−3378.
(69) Li, Z.; Brouwer, C.; He, C. *Chem. Rev.* **2008**, *108*, 3239−3265.
(70) Marion, N.; Nolan, S. P. *Chem. Soc. Rev.* **2008**, *37*, 1776−1782.
(71) Arduengo, A. J., III; Gamper, S. F.; Calabrese, J. C.; Davidson, F. *J. Am. Chem. Soc.* **1994**, *116*, 4391−4394.
(72) Böhm, V. P.; Gstöttmayr, C. W.; Weskamp, T.; Herrmann, W. A. *J. Organomet. Chem.* **2000**, *595*, 186−190.
(73) de Frémont, P.; Scott, N. M.; Stevens, E. D.; Ramnial, T.; Lightbody, O. C.; Macdonald, C. L.; Clyburne, J. A.; Abernethy, C. D.; Nolan, S. P. *Organometallics* **2005**, *24*, 6301−6309.
(74) Liu, B.; Ma, X.; Wu, F.; Chen, W. *Dalton Trans.* **2015**, *44*, 1836−1844.
(75) Lazreg, F.; Cordes, D. B.; Slawin, A. M.; Cazin, C. S. *Organometallics* **2015**, *34*, 419−425.
(76) F. A. Cotton, G. W. *Advanced Inorganic Chemistry*, 5th ed.; John Wiley & Sons, 1988; p 936.

DOI: 10.1021/acs.jctc.5b01166
J. Chem. Theory Comput. 2016, 12, 1236−1244